A New Method of Preparing Monolayers on Silicon and Patterning Silicon Surfaces by Scribing in the Presence of Reactive Species

ARTICLE *in* LANGMUIR · SEPTEMBER 2001

Impact Factor: 4.46 · DOI: 10.1021/la010017a

A New Method of Preparing Monolayers on Silicon and Patterning Silicon Surfaces by Scribing in the Presence of Reactive Species

Travis L. Niederhauser,† Guilin Jiang,† Yit-Yian Lua,† Michael J. Dorff,‡ Adam T. Woolley,† Matthew C. Asplund,† David A. Berges,† and Matthew R. Linford*,†

Department of Chemistry and Biochemistry, Brigham Young University, Provo, Utah 84602, and Department of Mathematics, Brigham Young University, Provo, Utah 84602

Received January 5, 2001. In Final Form: June 11, 2001

Here we describe a new and simple method for preparing alkyl monolayers on silicon, which consists of mechanically scribing oxide-coated silicon while it is wet with 1-alkenes or 1-alkynes (neat or in inert solvents) *under ambient conditions*. X-ray photoelectron spectroscopy, time-of-flight secondary ion mass spectrometry, wetting data, and stability tests suggest covalent bonding of unsaturated species to exposed silicon surfaces. Enclosures (hydrophobic corrals) made by scribing silicon that is wet with unsaturated hydrophobic species hold droplets of water and liquids with substantially lower surface tensions. Wetting tests suggest that 1-alkynes make better hydrophobic corrals than 1-alkenes, and theoretical results suggest it should be more difficult for alkyl chains of chemisorbed 1-alkenes to pack than those of 1-alkynes. Underivatized interior regions of hydrophobic corrals are functionalized with polyelectrolyte multilayers. Theoretical energies for water and methanol droplets (gravitational and surface) in hydrophobic corrals are calculated, and a model of failure of liquid droplets in hydrophobic corrals is presented.

Introduction

Here we describe a new method of modifying and patterning silicon. This technique consists of (a) cleaning a silicon wafer to remove adventitious contaminants from its surface, leaving its thin native oxide layer (10−15 Å thick), (b) wetting the dry surface of the clean silicon with an unsaturated, organic molecule, (c) mechanically scribing the silicon with a diamond-tipped instrument while it is wet with the unsaturated, organic liquid, and (d) cleaning the scribed surface to remove excess organic liquid and silicon particles that are produced by scribing. We show that monolayer quantities of alkyl chains are chemisorbed onto regions of silicon that are exposed by scratching when silicon is wet with a 1-alkene or a 1-alkyne (see Figure 1). Unlike other preparations of monolayers on silicon that require inert atmospheres, high vacuum conditions, or special equipment, this new technique can be performed under ambient conditions with minimal tools and supplies and without degassing or heating reagents. To our knowledge, this method is the first wet-chemical preparation of monolayers on silicon that does not require a hydrogen-terminated silicon intermediate. It also provides considerable flexibility in patterning silicon. We show that enclosures of scribed lines, or squares that are drawn on the silicon surface, which we call "hydrophobic corrals", hold droplets of water and other liquids. Moreover, the bare silicon oxide in the interior regions of hydrophobic corrals can be functionalized with polyelectrolyte multilayers, suggesting that this method can be used to partition and selectively derivatize silicon surfaces.

We hypothesize that the mechanism of formation of these new monolayers on silicon is closely related to the reaction of alkenes and alkynes with highly active surface species on unpassivated, bare silicon (see Figure 2). For example, the Si(111) (7 × 7) surface reacts with acetylene to form two silicon−carbon bonds.[1,2] Unpassivated Si(100) similarly reacts with acetylene,[3−5] ethylene,[4,6−9] propy-

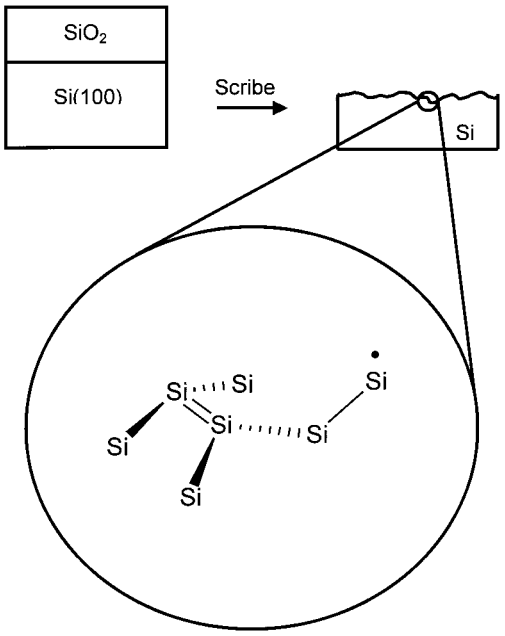

Figure 1. Scribing silicon to produce reactive species at fracture surfaces.

* E-mail: mrlinford@chemdept.byu.edu.
† Department of Chemistry and Biochemistry.
‡ Department of Mathematics.

(1) Yoshinobu, J.; Tsuda, H.; Onchi, M.; Nishijima, M. *Chem. Phys. Lett.* **1986**, *30*, 170−174.
(2) Hamers, R. J.; Wang, Y. *Chem. Rev.* **1996**, *96*, 1261−1290.
(3) Nishijima, M.; Yoshinobu, J.; Tsuda, H.; Onchi, M. *Surf. Sci.* **1987**, *192*, 383−397.
(4) Cheng, C. C.; Wallace, R. M.; Taylor, P. A.; Choyke, W. J.; Yates, J. T., Jr. *J. Appl. Phys.* **1990**, *67*, 3693−3699.
(5) Taylor, P. A.; Wallace, R. M.; Cheng, C. C.; Weinberg, W. H.; Dresser, M. J.; Choyke, W. J.; Yates, J. T., Jr. *J. Am. Chem. Soc.* **1992**, *114*, 6754−6760.

10.1021/la010017a CCC: $20.00
Published on Web 00/00/0000

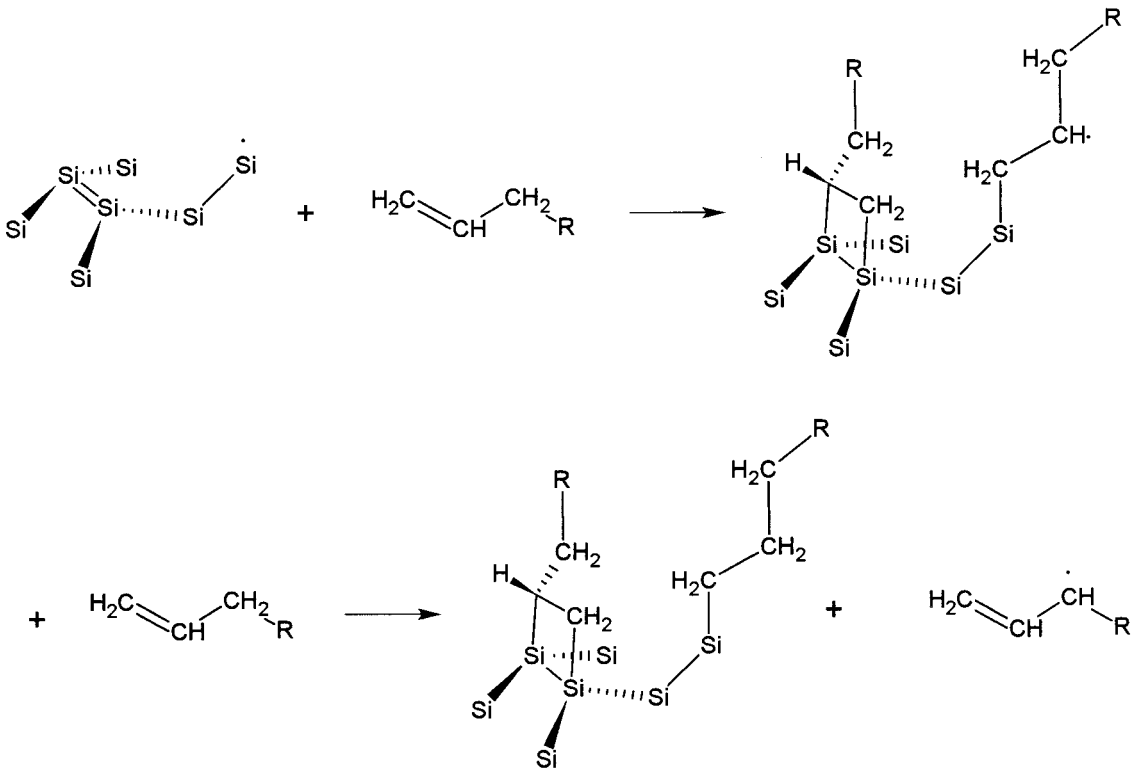

Figure 2. Possible reactions of reactive species on scribed silicon with a 1-alkene.

lene,[10,11] and other alkenes[12] to form two silicon−carbon bonds.[2,13−16] Neither methane nor propane reacts with annealed or ion roughened, unpassivated Si(100) at 120 K while propylene readily reacts under these conditions.[10] While the reaction of unsaturated organic compounds with scribed silicon is probably mechanistically similar to the reactions cited above on unpassivated silicon, our results suggest a close structural similarity between these new monolayers on silicon and alkyl monolayers on silicon[17−19] made from the reaction of 1-alkenes[20−24] and 1-alkynes[20,23,25,26] with hydrogen-terminated silicon. Alkyl monolayers formed from 1-alkenes on hydrogen-terminated silicon are robust; they are anchored through Si−C bonds[21] and are stable above 600 K in a vacuum.[27] Another important similarity between monolayers of alkyl chains on hydrogen-terminated silicon and these new monolayers is the "wet chemical" approach used in their preparation.

Other examples of chemical activation of materials through mechanical means include (a) removal of regions of alkanethiol monolayers on gold with micromachining techniques, i.e., a scalpel or carbon fiber, and exposure of the bare gold to a solution of a new thiol,[28] and (b) grinding silicon in the presence of 1-alkenes to create functionalized silicon particles.[29] The former procedure was used to create enclosures of hydrophobic lines of thiols on gold on a background of a hydrophilic thiol monolayer. These enclosures held water droplets. Triangular enclosures, which held droplets of alkane test liquids, were also made by this method, and a finite element analysis was performed of these drops.[30] We further note the growing interest in surface patterning, including hydrogen removal from hydrogen-terminated silicon via STM-induced excitations[31] to create dangling bonds that react with unsaturated species,[24] the development of soft lithography

(6) Yoshinobu, J.; Tsuda, H.; Onchi, M.; Nishijima, M. *J. Chem. Phys.* **1987**, *87*, 7332−7340.
(7) Cheng, C. C.; Choyke, W. J.; Yates, J. T., Jr. *Surf. Sci.* **1990**, *231*, 289−296.
(8) Mayne, A. J.; Avery, A. R.; Knall, J.; Jones, T. S.; Briggs, G. A. D.; Weinberg, W. H. *Surf. Sci.* **1993**, *284*, 247−256.
(9) Liu, H.; Hamers, R. J. *J. Am. Chem. Soc.* **1997**, *119*, 7593−7594.
(10) Bozack, M. J.; Taylor, P. A.; Choyke, W. J.; Yates, J. T., Jr. *Surf. Sci.* **1986**, *177*, L933-L937.
(11) Bozack, M. J.; Choyke, W. J.; Muehlhoff, L.; Yates, J. T., Jr. *Surf. Sci.* **1986**, *176*, 547−566.
(12) Hamers, R. J.; Hovis, J. S.; Lee, S.; Liu, H.; Shan, J. *Phys. Chem. B* **1997**, *101*, 1489−1492.
(13) Lopinski, G. P.; Moffatt, D. J.; Wayner, D. D. M.; Zgierski, M. Z.; Wolkow, R. A. *J. Am. Chem. Soc.* **1999**, *121*, 4532−4533.
(14) Lopinski, G. P.; Moffatt, D. J.; Wayner, D. D. M.; Wolkow, R. A. *J. Am. Chem. Soc.* **2000**, *122*, 3548−3549.
(15) Schwartz, M. P.; Ellison, M. D.; Coulter, S. K.; Hovis, J. S.; Hamers, R. J. *J. Am. Chem. Soc.* **2000**, *122*, 8529−8538.
(16) Hamers, R. J.; Coulter, S. K.; Ellison, M. D.; Hovis, J. S.; Padowitz, D. F.; Schwartz, M. P.; Greenlief, C. M.; Russell, J. N., Jr. *Acc. Chem. Res.* **2000**, *33*, 617−624.
(17) Linford, M. R.; Chidsey, C. E. D. *J. Am. Chem. Soc.* **1993**, *115*, 12631−12632.
(18) Buriak, J. M. *Chem. Commun.* **1999**, 1051−1060.
(19) Sieval, A. B.; Linke, R.; Zuilhof, H.; Sudhölter, E. J. R. *Adv. Mater.* **2000**, *12*, 1457−1460.
(20) Linford, M. R.; Fenter, P.; Eisenberger, P. M.; Chidsey, C. E. D. *J. Am. Chem. Soc.* **1995**, *117*, 3145−3155.
(21) Terry, J.; Linford, M. R.; Wigren, C.; Cao, R.-Y.; Pianetta, P.; Chidsey, C. E. D. *Appl. Phys. Lett.* **1997**, *71*, 1056−1058.
(22) Sieval, A. B.; Demirel, A. L.; Nissink, J. W. M.; Linford, M. R.; van der Maas, J. H.; de Jeu, W. H.; Zuilhof, H.; Sudhölter, E. J. R. *Langmuir* **1998**, *14*, 1759−1768.
(23) Bateman, J. E.; Eagling, R. D.; Worrall, D. R.; Horrocks, B. R.; Houlton, A. *Angew. Chem., Int. Ed. Engl.* **1998**, *37*, 2683−2685.
(24) Lopinski, G. P.; Wayner, D. D. M.; Wolkow, R. A. *Nature* **2000**, *406*, 48−51.
(25) Cicero, R. L.; Linford, M. R.; Chidsey, C. E. D. *Langmuir* **2000**, *16*, 5688−5695.
(26) Sieval, A. B.; Opitz, R.; Maas, H. P. A.; Schoeman, M. G.; Meijer, G.; Vergeldt, F. J.; Zuilhof, H.; Sudhölter, E. J. R. *Langmuir* **2000**, *16*, 10359−10368.
(27) Sung, M. M.; Kluth, G. J.; Yauw, O. W.; Maboudian, R. *Langmuir* **1997**, *13*, 6164−6168.
(28) Abbott, N. L.; Folkers, J. P.; Whitesides, G. M. *Science* **1992**, *257*, 1380−1382.
(29) Linford, M. R. Producing coated particles by grinding in the presence of reactive species. U.S. Patent 6,132,801, 2000.
(30) Abbott, N. L.; Whitesides, G. M.; Racz, L. M.; Szekely, J. *J. Am. Chem. Soc.* **1994**, *116*, 290−294.
(31) Avouris, Ph.; Walkup, R. E.; Rossi, A. R.; Akpati, H. C.; Nordlander, P.; Shen, T.-C.; Abeln, G. C.; Lyding, J. W. *Surf. Sci.* **1996**, *363*, 368−377.

techniques,[32] which have been used to pattern surfaces with monolayers that have different surface free energies,[33] and surface patterning of lipid bilayers to form corrals on glass using both lines of barrier materials[34] and lines scratched on glass at basic pH.[35,36]

This work was undertaken both as a fundamental study of the reactivity of bare silicon fracture surfaces and also to develop new methods of patterning silicon surfaces. X-ray photoelectron spectroscopy (XPS) and wetting data show that when silicon is first scribed in the air and then wet with a reactive compound, no reaction takes place. However, when silicon is wet with a reactive compound and then scribed, monolayer quantities of alkyl chains are deposited. Time-of-flight secondary ion mass spectrometry (TOF-SIMS) shows numerous fragments that contain C and H as well as many fragments with Si, C, and H. These latter species suggest covalent attachment of alkyl chains to surfaces.

Hydrophobic corrals were probed with test droplets of methanol−water mixtures. The surface tensions of methanol−water mixtures that are held by hydrophobic corrals and the amount of carbon observed by XPS are proportional to the number of carbons in the unsaturated species from which the hydrophobic corral is prepared. While XPS shows that the amount of chemisorbed carbon is the same for 1-alkenes and 1-alkynes with the same number of carbons, wetting results suggest that 1-alkynes form better hydrophobic corrals than 1-alkenes. Theoretical studies predict a difference in the orientation of alkyl chains of 1-alkenes and 1-alkynes that are bonded through two carbon−silicon bonds to silicon. Hydrophobic corrals made from a fluorinated alkene hold test droplets with lower surface tensions than hydrogenated 1-alkenes and 1-alkynes. Monolayers on silicon can be prepared from neat compounds or from 1-alkenes and 1-alkynes that are dissolved in an inert solvent. To demonstrate selective functionalization of interior regions of hydrophobic corrals, polyelectrolyte multilayers were sequentially deposited, as measured by variable angle spectroscopic ellipsometry. A finite element analysis of water and methanol droplets in hydrophobic corrals was performed. A function that describes the drop shapes and predicts their energies in a computationally simple fashion is also presented, and the difference between the surface tensions at the hydrophobic line−air interface and the hydrophobic line−liquid interface of a model system is predicted.

Experimental Section

Materials. The following chemicals were obtained from Aldrich and used as received: 1-pentene (99%), 1-octene (98%), 1-dodecene (95%), 1-hexadecene (92%), $CH_2{=}CH(CF_2)_5CF_3$ (99%), 1-pentyne (99%), 1-octyne (97%), 1-dodecyne (98%), octane (99+%), dodecane (99+%), $CF_3(CF_2)_6CF_3$ (98%), polyethylenimine (50 wt % solution, $M_w \sim 750\,000$), poly(sodium 4-styrene sulfonate) ($M_w \sim 70\,000$), poly(allylamine hydrochloride) ($M_w \sim 70\,000$). Acetone and *m*-xylene were reagent grade, and water was obtained from a Millipore Milli-Q water system. Glycerol (Certified A.C.S., Fisher Scientific), ethylene glycol (Analytical Reagent, Mallinckrodt), and sodium dodecyl sulfate (NF Grade, Columbus Chemical Industries) were used as received. Silicon (100) wafers (p-boron, 0−100 Ω cm, test grade) were obtained from TTI Silicon (Sunnyvale, CA).

Silicon Cleaning. Silicon surfaces were cleaned[37] by immersion in ~50:50 (v/v) H_2O_2 (30%):NH_4OH (concentrated) for 30−45 min at room temperature and then rinsed with copious amounts of water. *Warning: mixtures of concentrated H_2O_2 and NH_4OH are exceedingly caustic and should be handled with great care.* After the surfaces were cleaned and dried with a jet of N_2, the silicon surfaces were completely hydrophilic. H_2O_2/NH_4OH cleaning solutions were carefully neutralized with a concentrated solution of citric acid before disposal.

Sample Preparation. All sample preparations were done in the air with compounds that had not been degassed. To obtain surfaces for XPS and TOF-SIMS analyses, silicon surfaces were cleaned and rinsed as described above, dried with a jet of nitrogen, wet with an organic liquid, and scribed (by hand) with a broad, diamond-tipped machining tool over a region large enough (~1 cm^2) to easily accommodate XPS and TOF-SIMS probe beams. For a few of the surfaces, this process was automated by using a spring-loaded diamond-tipped rod that was held and moved by three orthogonally mounted computer-controlled translation stages (Coherent). After the surface was wetted with a reactive compound, lines were drawn 50 μm apart in one direction to cover a region of interest and this same rastering was then performed perpendicular to the original direction. The diamond-tipped rod was obtained from a diamond scriber sold by VWR (catalog no. 52865-005). (After repeated use, diamond tips begin to degrade and may produce double lines on silicon.) Three Labmotion series 640 Linear SmartStages (catalog no. 61-7225) were connected to a controller chassis with LabMotion stepper drive modules SDM-1, which was in turn controlled through the LabMotion Designer Software.

Hydrophobic corrals were made by scribing silicon, which had been wet with a reactive liquid, with a spring-loaded diamond tip in a custom-designed holder that was attached to and moved by a computer numerically controlled (CNC) Fryer MB15 bed mill. A program instructed the machine to make 5 horizontal and 5 vertical lines 0.5 cm apart, i.e., 16 corrals.

After the surfaces were scribed, samples were rinsed with copious amounts of acetone followed by water, were cleaned by rubbing with a soft artist's brush and a 2% sodium dodecyl sulfate solution, and were finally rinsed again with copious amounts of water. The use of a brush and a detergent solution to clean siloxane monolayer surfaces has previously been reported.[38] In a few cases, surfaces were gently rubbed with a gloved hand instead of a brush during the cleaning process. After the samples were cleaned, surfaces were dried with a jet of nitrogen. After exposure to the laboratory environment for many days, hydrophilic regions on silicon surfaces became hydrophobic.

For interior region functionalization, hydrophobic corrals were made fairly large (1.5 × 1.5 cm^2) to accommodate the footprint of an ellipsometer light beam. These hydrophobic corrals were produced by scribing silicon in the presence of 1-hexadecene and were found to easily hold 400 μL droplets of water, which was the volume used in surface functionalizations with polyelectrolytes. In the first step of the derivitization, 400 μL of water was added to a hydrophobic corral with a micropipettor. Next, 300 μL of the 400 μL water droplet was removed with a micropipettor and replaced with 300 μL of an aqueous solution of a polyelectrolyte (1.33 mM in monomer) making the solution above the surface 1 mM (in monomer).

After 30 min was allowed for the adsorption of the initial layer of polyethylenimine (PEI) and 20 min for subsequent layers of poly(sodium 4-styrenesulfonate) (PSS) or poly(allylamine) hydrochloride (PAH), 300 μL of the 400 μL 1 mM polyelectrolyte solution was removed and replaced with 300 μL of water. This rinse was repeated five times, lowering the concentration above the surface to less than 0.1% of its original value, where complete mixing was assumed. Next, 300 μL of the drop was removed and replaced with the next 1.33 mM polymer solution. With each addition, liquid was repeatedly sucked up into the tip of the micropipettor and reinjected into the droplet over the hydrophobic

(32) Xia, Y.; Whitesides, G. M. *Angew. Chem., Int. Ed.* **1998**, *37*, 550−575.
(33) Gorman, C. B.; Biebuyck, H. A.; Whitesides, G. M. *Chem. Mater.* **1995**, *7*, 252−254.
(34) Groves, J. T.; Ulman, N.; Boxer, S. G. *Science* **1997**, *275*, 651−653.
(35) Cremer, P. S.; Groves, J. T.; Kung, L. A.; Boxer, S. G. *Langmuir* **1999**, *15*, 3893−3896.
(36) Groves, J. T.; Ulman, N.; Cremer, P. S.; Boxer, S. G. *Langmuir* **1998**, *14*, 3347−3350.
(37) Kern, W.; Puotinen, D. A. *RCA Rev.* **1970**, *31*, 187−206.
(38) Tillman, N.; Ulman, A.; Schildkraut, J. S.; Penner, T. L. *J. Am. Chem. Soc.* **1988**, *110*, 6136−6144.

corral to mix the liquids. In this manner, the region inside the hydrophobic corral was altered without affecting the surrounding surface.

Instrumentation. X-ray photoelectron spectroscopy (XPS) (VG Eclipse 220i-XL) was performed with a monochromatic Al Kα X-ray source and with an electron takeoff angle of 90°. In analyses of XPS data, which were performed with the instrument software, it was assumed that all of the carbon on the surface comes from the unsaturated species and no attempt was made to account for attenuation of photoelectrons.[39]

Static time-of-flight secondary ion mass spectrometry (*TOF-SIMS*) (Cameca/ION-TOF TOF−SIMS IV) was performed with a monoisotopic 25 keV $^{69}Ga^+$ primary ion source in "bunched mode" to achieve a mass resolution of ~10 000 ($m/\Delta m$). The primary ion (target) current was typically 3 pA, with a pulse width of 20 ns before bunching, and the raster area of the beam was 500 × 500 μm^2.

Variable angle spectroscopic ellipsometry (M-44, J. A. Woollam Co.) was performed at 44 wavelengths between 286.1 and 605.2 nm, inclusive. Optical constants in instrument software files (SIO2.MAT and si_jaw.mat), which had been obtained from the literature,[40,41] were used to model silicon oxide and silicon. The thicknesses of the single PEI layers reported at the end of the results section were obtained with an M-2000 variable angle spectroscopic ellipsometer (J.A. Woollam Co.), which takes 498 data points from 190.51 to 989.43 nm, inclusive. The mean squared error (MSE) for all of the ellipsometric measurements, which measures the goodness of fit to the ellipsometry data, is given in the instrument software as

$$\mathrm{MSE} = \left\{\frac{1}{2N-M}\sum_{i=1}^{N}\left[\left(\frac{\Psi_i^{\mathrm{model}}-\Psi_i^{\mathrm{exptl}}}{\sigma_{\Psi,i}^{\mathrm{exptl}}}\right)^2+\left(\frac{\Delta_i^{\mathrm{model}}-\Delta_i^{\mathrm{exptl}}}{\sigma_{\Delta,i}^{\mathrm{exptl}}}\right)^2\right]\right\}^{1/2} \quad (1)$$

where Ψ^{exptl} and Δ^{exptl} are the measured values of Ψ and Δ and Ψ^{model} and Δ^{model} are those predicted by a user-defined model. The symbol σ gives the standard deviation of either Ψ or Δ at a given wavelength, so that less precise data receives less weight in the fit. N is the number of $\Psi-\Delta$ pairs that are measured, and M is the number of real-valued fit parameters. Models were created and data analyzed with the instrument software. The mean squared errors (MSE) of all fits of models to experimental data were less than 5, which is generally considered to be an excellent fit.

Scanning electron microscopy (SEM) was performed with a JEOL JSM 840A instrument. Profilometry was performed with an Alpha-Step 200 profilometer. The stylus can be modeled as a 60° cone rounded to a spherical tip with a 12.5 μm radius.

Atomic force microscopy (AFM) was carried out using a Digital Instruments (Santa Barbara, CA) Multimode Nanoscope IIIa instrument operating in contact mode with etched Si tips and an imaging setpoint of 2.0 V. Height images were modified with a zero order flatten and first order planefit to account for the difference between the plane of the sample and that of the piezoelectric scanner. Image analysis was performed offline using the roughness and section commands provided in the AFM software.

Methanol−Water Mixtures for Probing Hydrophobic Corral Wetting Properties. Various mixtures of alcohols in water with a range of surface tensions, along with the homologous series of alkanes, including hexadecane, tetradecane, dodecane, etc., are commonly used in the textile industry as a rapid and inexpensive probe of the surface tensions of fabrics and their chemical finishes, e.g., water and oil repellent treatments. By use of this method, droplets of liquids with progressively lower surface tensions are placed on a fabric until they are observed to wet or even fully penetrate a material. Here we similarly use a series of methanol−water mixtures that have different surface tensions as a means of comparing the hydrophobicity of functionalized lines that make up hydrophobic corrals.

An equation relating the surface tension of a methanol−water mixture to its percent (by volume) of methanol was obtained by linearly interpolating literature data to 25 °C[42] and by then fitting the results to a polynomial. The following empirical equation gives an excellent fit to the data over its range (7.5%−100% (v/v) methanol in water):

$$\gamma_{\mathrm{MeOH/water\ solution}} = -5.71\times10^{-5}V_{\%\mathrm{MeOH}}{}^3 + 0.0126V_{\%\mathrm{MeOH}}{}^2 - 1.16V_{\%\mathrm{MeOH}} + 68.2 \quad (2)$$

The wetting properties of hydrophobic corrals were probed by placing 20 μL of a methanol−water test mixture into a hydrophobic corral using a 25 μL syringe (Hamilton Co., Reno, NV). If the test droplet was held by, and did not overrun the boundaries of, the hydrophobic corral, the droplet was considered to pass. The tip of the needle that dispensed the liquid was not removed from the drop during the testing process because the shock of removing it sometimes caused droplets with low surface tensions to fail. If the probe liquid did not pass the first time, the experiment was repeated. If it did not pass the second time, the liquid was considered to fail. After being tested with a probe liquid, the sample was rinsed with water and dried with a jet of N_2. Test droplets (20 μL) of glycerol and ethylene glycol were dispensed with a micropipettor. At least eight different hydrophobic corrals were tested and the results averaged under each set of conditions described in this work.

Finite element analysis was performed with the Surface Evolver program, which is an interactive program for modeling liquid surfaces shaped by various forces and constraints. Surface tensions of 71.99 and 22.07 mN/m and densities of 0.9970 and 0.7855 g/cm^3 for water and methanol, respectively, were employed.[42] The datafile "mound.fe," which models a mound of liquid sitting on a tabletop with gravity acting on it and which accompanies Surface Evolver, was modified to form a parallelpiped with a square base in which each edge has length 0.5 cm and a height of 0.08 cm, so that its volume is 20 μL. The base edges and base vertexes were fixed, and the gravity constant was set to 980. Surface Evolver was then run on this datafile, refining it and iterating until the desired accuracy was acheived. In this manner the drop shape was minimized with respect to the surface energy at the liquid−vapor interface and the gravitational energy.[30] The total energy is the sum of the gravitational energy of the drop, with the base of the drop as the zero of energy, and the energy contribution from the liquid−air surface area of the drop. The program was written by K. A. Brakke as part of the Geometry Supercomputing Project (now The Geometry Center), sponsored by the National Science Foundation, the Department of Energy, Minnesota Technology, Inc., and the University of Minnesota. The source code is written in C and runs on many systems. Surface Evolver and documentation are available free of charge on the Internet at http://www.geom.umn.edu/software/evolver/.

Theoretical Calculations. The silicon (100) surface was modeled as a cluster of 48 Si atoms arranged in a tetrahedral structure and terminated with hydrogen atoms. 1-Dodecene and 1-dodecyne were attached to the center of the (100) face of the cluster with their free alkyl chains in an all-trans conformation, which is typical for monolayers of alkyl chains on gold,[43] silicon oxide,[44] and silicon,[20,45] and the geometry was optimized with an MMFF94 force field and with the PM3 semiempirical method using the program Spartan (PC Spartan Plus 1.5.2, Wavefunction, Inc., 18401 Von Karman Ave., Ste. 370, Irvine, CA 92612). The structures from the PM3 calculations were used as the initial guess for ab initio calculations with Gaussian 98 (Gaussian 98 revision A.6, Gaussian Inc., Carnegie Office Park, Building 6,

(39) Bain, C. D.; Whitesides, G. M. *J. Phys. Chem.* **1989**, *93*, 1670−1673.
(40) Herzinger, C. M.; Johs, B.; McGahan, W. A.; Woollam, J. A.; Paulson, W. *J. Appl. Phys.* **1998**, *83*, 3323−3336.
(41) *Handbook of Optical Constants of Solids*; Academic Press: San Diego, 1998.
(42) *Handbook of Chemistry and Physics*; CRC Press: Boca Raton, 2000.
(43) Porter, M. D.; Bright, T. B.; Allara, D. L.; Chidsey, C. E. D. *J. Am. Chem. Soc.* **1987**, *109*, 3559−3568.
(44) Maoz, R.; Sagiv, J. *J. Colloid Interface Sci.* **1984**, *100*, 465−496.
(45) Sieval, A. B.; van den Hout, B.; Zuilhof, H.; Sudhölter, E. J. R. *Langmuir* **2000**, *16*, 2987−2990.

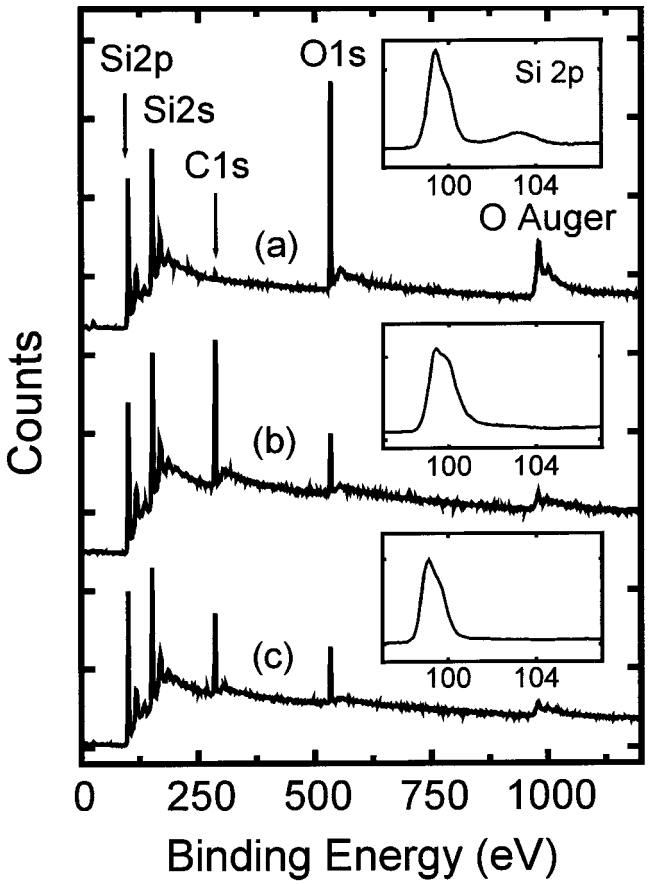

Figure 3. XPS spectra of silicon: (a) scribed in air and then wet with 1-dodecene; (b) scribed while wet with 1-dodecene; (c) scribed while wet with 1-octyne.

Suite 230, Carnegie, PA 15106) using a Hartree−Fock STO-3G basis set. This result was then used as the initial guess for the next level of theory (Hartree−Fock 3-21G* basis set).

Results

Overview. The first part of this section contains XPS, TOF-SIMS, and wetting evidence for monolayer formation on silicon that is scribed in the presence of unsaturated organic liquids. The second part shows how patterns of hydrophobic lines that form enclosures on silicon surfaces, or hydrophobic corrals, can be made and characterized and how their interior regions can be functionalized. The third part contains the results of finite element analyses of methanol and water droplets in hydrophobic corrals and also gives a mathematical analysis of drop failure in hydrophobic corrals. Finally, a theoretical study of unsaturated adsorbates on silicon is presented.

A. XPS, TOF-SIMS, and Wetting of Monolayers on Silicon Prepared by Scribing in the Presence of 1-Alkenes, Including CH_2=$CH(CF_2)_5CF_3$, and 1-Alkynes. The consequences of scribing silicon in the presence of unsaturated species were studied by XPS and TOF-SIMS.[46] Figure 3 shows XPS survey spectra and accompanying Si 2p narrow scans (insets) of (a) a control experiment in which dry, clean silicon was first scribed in the air and then wet with 1-dodecene, (b) silicon that was wet with 1-dodecene and then scribed, and (c) silicon that was wet with 1-octyne and then scribed. The control surface (Figure 3a) shows a weak C 1s signal, strong oxygen 1s and Auger signals, and a chemically shifted Si 2p peak at ∼103 eV, which indicates silicon oxide (see inset to Figure 3a).[47] XPS spectra from other control experiments, including dry silicon scribed in the air and dry silicon scribed in the air and then wet with 1-octyne, are virtually identical to Figure 3a. Spectra b and c of Figure 3 show that when silicon is wet with an unsaturated species and then scribed, less oxygen is found on the surface than when the surface is scribed in air, a significant carbon signal appears that corresponds to monolayer quantities of alkyl chains,[25,48,49] and significantly less silicon oxide is observed (Si 2p narrow scan insets) than when silicon is first scribed in the air.

It is expected, based on numerous wetting studies of alkyl monolayers[50] on gold,[51,52] silicon oxide,[44] and silicon,[20,53] that if monolayer quantities of alkyl chains chemisorb onto silicon by the methods described here, the resulting surfaces should be hydrophobic. It is also expected that bare silicon oxide surfaces should be hydrophilic. In agreement with these predictions, water beads up on and runs off of silicon surfaces that are scribed in the presence of 1-alkenes and 1-alkynes. Control surfaces that were made by scribing dry silicon in the air, with or without subsequent addition of an unsaturated compound, are indeed hydrophilic.

Figure 4, which shows XPS data of surfaces that were prepared by scribing silicon in the presence of a series of 1-alkenes and 1-alkynes with different chain lengths, reveals three important features of this system. First, in the range of alkyl chain lengths studied, the ratio of the area of the C 1s to the Si 2p XPS peaks, which is a measure of the amount of carbon on the surface, depends linearly on the number of carbon atoms in the 1-alkene or 1-alkyne. Second, to within experimental error, the amount of carbon deposited on the surface is the same for 1-alkenes (solid squares) and 1-alkynes (solid triangles) with the same number of carbon atoms. Third, the number of oxygen atoms on the surface per alkyl chain (2.28 ± 0.35) (open symbols) is independent of the number of carbon atoms in the unsaturated species.

Compounds containing fluorinated alkyl chains often have unique characteristics, including chemical inertness and low surface tensions.[50,54] In an effort to impart some of these properties to silicon surfaces, dry silicon substrates were wet with CH_2=$CH(CF_2)_5CF_3$ and then scratched with a diamond-tipped instrument. As expected, the resulting surfaces were hydrophobic. The C1s/Si2p ratio and the number of oxygen atoms per alkyl chain by XPS for these surfaces are 0.47 ± 0.01 and 3.3 ± 0.1, respectively. This C 1s/Si 2p ratio is lower than that for 1-octene and 1-octyne (∼0.67) and approximately equal to the value for 1-pentene and 1-pentyne (∼0.49) (see Figure 4). Factors contributing to the lower carbon and higher oxygen levels in these surfaces may be (1) the larger diameter of fluorinated alkyl chains as opposed to normal alkyl chains and (2) the

(46) Ulman, A. *Characterization of Organic Thin Films*; Butterworth-Heinemann: Woburn, MA, 1994.

(47) Moulder, J. F.; Stickle, W. F.; Sobol, P. E.; Bomben, K. D. *Handbook of X-ray Photoelectron Spectroscopy*; Physical Electronics, Inc.: Eden Prarie, MN, 1995.

(48) Bansal, A.; Li, X.; Lauermann, I.; Lewis, N. S. *J. Am. Chem. Soc.* **1996**, *118*, 7225−7226.

(49) Wagner, P.; Nock, S.; Spudich, J. A.; Volkmuth, W. D.; Chu, S.; Cicero, R. L.; Wade, C. P.; Linford, M. R.; Chidsey, C. E. D. *J. Struct. Biol.* **1997**, *119*, 189−201.

(50) Ulman, A. *An Introduction to Ultrathin Organic Films from Langmuir−Blodgett to Self-Assembly*; Academic Press: Boston, 1991.

(51) Bain, C. D.; Troughton, E. B.; Tao, Y.-T.; Evall, J.; Whitesides, G. M.; Nuzzo, R. G. *J. Am. Chem. Soc.* **1989**, *111*, 321−335.

(52) Bain, C. D.; Whitesides, G. M. *J. Am. Chem. Soc.* **1989**, *111*, 7164−7175.

(53) Sieval, A. B.; Vleeming, V.; Zuilhof, H.; Sudhölter, E. J. R. *Langmuir* **1999**, *15*, 8288−8291.

(54) Li, D.; Neumann, A. W. *J. Colloid Interface Sci.* **1992**, *148*, 190−200.

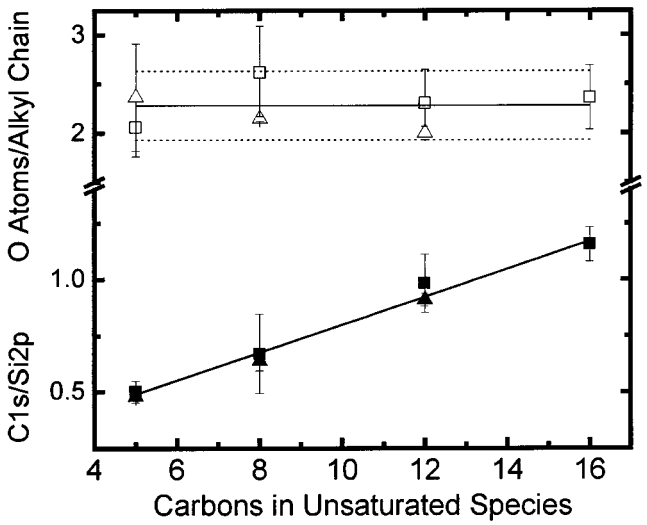

Figure 4. Ratio of the raw carbon peak area to raw silicon peak area by XPS and the number of oxygen atoms per alkyl chain, which is the product of the number of carbon atoms in the alkyl chain multiplied by the normalized O peak area divided by the normalized C peak area. Results shown were obtained from 18 surfaces: 1-alkene surfaces (squares) were made three times, and 1-alkyne surfaces (triangles) were made twice. The C 1s/Si 2p data are given by solid symbols, and the O atoms/alkyl chain data by open symbols. The fit to the C 1s/Si 2p data is the line passing through the solid symbols and is given by C 1s/Si 2p = 0.062 * (number of carbons in the unsaturated species) + 0.18.

lack of an allylic hydrogen in $CH_2{=}CH(CF_2)_5CF_3$. (The numerical values given in this and the next paragraph are the average values from two experiments and the error is half of the difference between the data points.)

Control surfaces were also characterized by XPS. Dry silicon that was scratched in the air (see Figure 3a) had a C 1s/Si 2p ratio of 0.06 ± 0.02. For silicon surfaces that were scribed in the air and then wet with 1-dodecene or 1-octyne, the C 1s/Si 2p ratios are 0.07 ± 0.01 and 0.09 ± 0.02, respectively, while the O/alkyl chain ratios are 97 ± 20 and 50 ± 8, respectively. As expected, the C 1s/Si 2p ratio is much lower and the O/alkyl chain ratio is substantially higher for the controls than for silicon surfaces scribed in the presence of unsaturated species (see Figure 4).

Static TOF-SIMS positive ion spectra of silicon scribed in the presence of 1-octene, 1-dodecene, 1-hexadecene, 1-octyne, and 1-dodecyne were obtained. Significant fragmentation of surface species would be expected because the energy of the primary ion source (25 keV Ga^+) is more than 6000 times the strength of a typical covalent bond (~4 eV). All of the spectra contain a variety of masses that correspond to hydrocarbon fragments (combinations of ^{12}C and ^{1}H) including C_nH_{2n} (n = 1−5), C_nH_{2n+1} (n = 1−6), $C_{n+1}H_{2n-2}$ (n = 2−4), $C_{n+1}H_{2n}$ (n = 1−4), $C_{n+1}H_{2n+1}$ (n = 0−5), $C_{n+2}H_{2n-1}$ (n = 1−4), and $C_{n+2}H_{2n+1}$ (n = 0−5), as well as masses that suggest combinations of ^{28}Si, ^{12}C, and ^{1}H such as SiC_nH_n (n = 1−4), SiC_nH_{2n} (n = 1−4), SiC_nH_{2n+1} (n = 1−4), SiC_nH_{2n+3} (n = 1−2), $SiC_{n+1}H_{2n+1}$ (n = 1−3), $SiC_{n+2}H_{2n+1}$ (n = 0−3), Si_2CH, and Si_2C_2H. The fragments that contain Si, C, and H are suggestive of covalent bonding of alkyl chains to the silicon surface. Nevertheless, the possibility that atomic and/or molecular fragments may combine in the high pressure region immediately above the sample to produce some of the results observed cannot be eliminated at present. Either

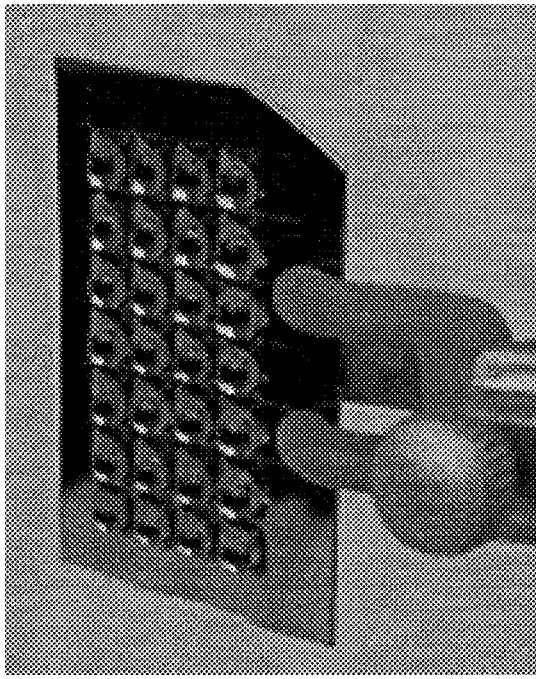

Figure 5. Water droplets held in a set of 28 hydrophobic corrals produced by scribing Si(100) in the presence of 1-hexadecene. After the initial cleaning with acetone and water, the corral interiors were perfectly hydrophilic. After stability tests, unscribed regions were somewhat hydrophobic, water no longer wet them perfectly, but water droplets are still unable to escape from hydrophobic corrals, even when the sample is turned on its side, as shown.

Si^+ or SiH^+ was the base peak (most intense feature) in all of the spectra, and Si_2^+ is also present in all of the spectra.

B. Formation of Hydrophobic Corrals from Neat and Diluted Compouds and Wetting of and Functionalization in Hydrophobic Corrals. 1. Formation of Hydrophobic Corrals. Up to this point we have described the characterization of small patches of scribed silicon, which were large enough to accommodate the XPS X-ray spot size. Here we focus on checkerboard patterns of lines that are drawn on silicon that is wet with unsaturated organic compounds. Water springs back from these lines, and the square enclosures of the array, hydrophobic corrals, hold individual droplets of water. The interior regions of hydrophobic corrals remain hydrophilic (unfunctionalized) after corral preparation.

Figure 5 shows 28 water droplets in a grid of hydrophobic lines, 0.5 cm apart, on a silicon surface, which has been turned on its side (vertically). The surface was prepared by scratching silicon that was wet with 1-hexadecene with a diamond scribe. Following an initial cleaning by rinsing with copious amounts of acetone and water, the surface was exposed overnight to recirculated hot *m*-xylene (bp 138 °C) in a Soxhlet extractor, highly efficient degreasing conditions, and then immersed in boiling water for 1 h. That the individual hydrophobic corrals still hold distinct water droplets after these stability experiments, even in the geometry shown, shows a high level of stability of these monolayer coatings and further suggests covalent surface attachment of 1-hexadecene to silicon.

Scanning electron microscopy shows that the width of scribed lines is 50−100 μm and that their interiors and edges are rough (Figure 6). Profilometry also indicates that the lines are rough and puts a lower limit on their depth (4.2 ± 1.4 μm). A more thorough characterization of scribed surfaces by atomic force microscopy shows that

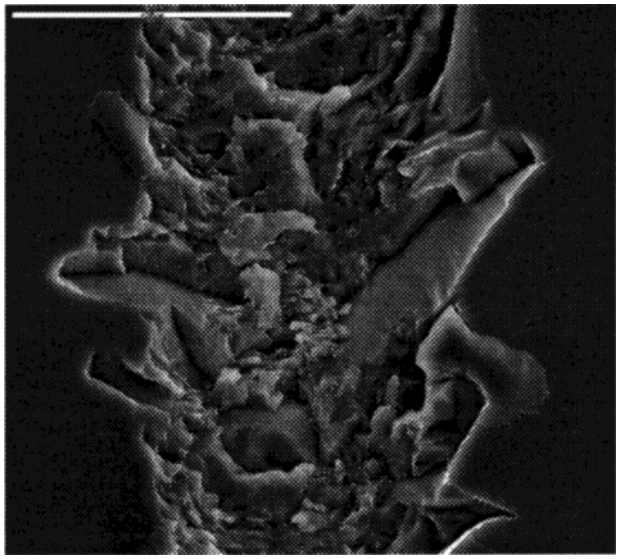

Figure 6. SEM picture of a functionalized line on silicon (the white bar in the upper left corner is 50 μm long).

the roughened surface features vary in width from ~100 nm to >5 μm and that these bumps have a low height-to-width ratio (typically 1:10 and infrequently greater than 1:5). Some relatively flat areas (as large as 10 μm^2) are occasionally observed (see Figure 7); the root-mean-square roughness of these areas is as low as 7 nm for a 2.5 μm × 2.5 μm region with 50 nm height range. The depth of scribed lines varies from as small as 1 μm to greater than the range of the scanner (5.5 μm).

2. Wetting Properties of Hydrophobic Corrals. To quantify the wetting properties of hydrophobic corrals made from a variety of unsaturated compounds, 0.5 × 0.5 cm^2 square hydrophobic corrals (see Figure 5) were tested with a series of 20 μL droplets of methanol−water mixtures that had surface tensions that decreased progressively in steps of 2−3 mJ/m^2 from 71.99 (water) down to 22.07 mJ/m^2 (methanol). An advantage of using methanol−water mixtures is the ease with which a series of liquids with a range of surface tensions can be prepared. A disadvantage of using such a two-component system in wetting studies[55] is that it does not allow an empirical equation of state[56] of the form $\gamma_{sl} = f(\gamma_{sv},\gamma_{lv})$ to be used to determine γ_{sl} and γ_{sv}. Hydrophobic corrals were probed by determining the lowest surface tension of a droplet that could be held by a corral (passing) and the highest surface tension of a droplet that overran the scribed lines (failing). To prepare test corrals that were as uniform as possible, the scribing process was automated (see the Experimental Section).

Figure 8 shows plots of the average passing and failing surface tensions of 20 μL test droplets of methanol−water mixtures, glycerol, and ethylene glycol in 0.5 × 0.5 cm^2 hydrophobic corrals (see also Figure 9), which were made by scribing silicon in the presence of 1-alkenes and 1-alkynes with 5, 8, 12, and 16 carbons. As would be expected if these compounds were reacting with the silicon surface to form monolayers, the passing surface tension of a methanol−water droplet in a corral decreases with increasing chain length of the unsaturated species. With the exception of the corral made with 1-pentene, all of the hydrophobic corrals in Figure 8 hold 20 μL droplets of glycerol, which has a surface tension of 64 mJ/m^2.[57] None of the hydrophobic corrals that are derived from 1-pentene, 1-octene, or 1-pentyne hold 20 μL droplets of ethylene glycol, which has a surface tension of 48 mJ/m,[2,57] while those prepared from the other 1-alkenes and 1-alkynes, including 1-octyne, do. A comparison of the wetting results for 1-alkenes and 1-alkynes in Figure 8 suggests that 1-alkynes make more hydrophobic corrals than 1-alkenes.

Finally, we note that corrals made with a fluorinated 1-alkene ($CH_2{=}CH(CF_2)_5CF_3$) hold methanol−water droplets with even lower surface tensions (passing, 27 ± 1; failing, 24 ± 1) than any of the corrals shown in Figure 8. They also hold 20 μL droplets of glycerol and ethylene glycol. These results are consistent with the fact that $-CF_2-$ and $-CF_3$ groups have some of the lowest surface tensions known.[50]

3. Dilution of Unsaturated Compounds in Inert Solvents. It would be advantageous to dilute compounds that must be synthesized because of lack of commercial availability or that are expensive rather than to employ neat liquids in silicon modification by scribing.[53] It seems reasonable that alkanes, e.g., octane and dodecane, might function as inert solvents because it is known that propane and methane do not react with ion-roughened silicon at low temperature.[10] Perfluorooctane was also studied as a possible inert solvent. Hydrophobic corrals prepared by scribing silicon that was wet with octane, dodecane, and perfluorooctane did not hold 20 μL water droplets. However, these lines did have low levels of hydrophobicity, which may be due to small amounts of unsaturated impurities.

Figure 10 shows the passing and failing surface tensions of 20 μL methanol−water, glycerol, and ethylene glycol test droplets in hydrophobic corrals, which were prepared by scribing silicon in the presence of 1-dodecene and 1-octyne at 100%, 10%, 1%, and 0.1% (v/v) dilution in dodecane. The results at 100% (neat compounds) and 10% dilution are nearly the same. However, at 1% and to a greater extent at 0.1% dilution, the hydrophobic corrals begin to lose their ability to hold test droplets with low surface tensions. Nevertheless, unlike hydrophobic corrals formed with dodecane, those made with 0.1% 1-dodecene and 1-octyne still have not completely lost their ability to hold methanol−water or glycerol test droplets.

A possible explanation for the trend shown in Figure 10 is that dissolved oxygen begins to compete effectively with 1-alkenes and 1-alkynes, when their concentrations are sufficiently low. Indeed, at 0.1% (v/v) dilution in dodecane, the concentrations of 1-dodecene (4.5 mM) and 1-octyne (6.8 mM) are relatively close to that of oxygen in hydrocarbons: ~2 mM, an estimate based on the solubility of oxygen in decane,[58] using dodecane's physical constants, and assuming 21% oxygen in the air and that the different liquid volumes in the mixtures are additive. If this explanation is correct, it suggests similar reaction rates for oxygen, 1-alkenes, and 1-alkynes with scribed silicon.

4. Interior Surface Functionalization of Hydrophobic Corrals. When hydrophobic corrals are prepared, only the scribed lines are functionalized, and not the unmarked silicon/silicon oxide. We propose that it will be possible to create arrays of functionalized hydrophobic corrals, where each may have a unique surface coating and that these may prove useful in studying and optimizing a variety of surface properties and reactions. Here we use polyelectrolyte multilayer deposition[59] to show that

(55) Li, D.; Ng, C.; Neumann, A. W. *J. Adhesion Sci.. Technol.* **1992**, *6*, 601.
(56) Li, D.; Neumann, A. W. *Adv. Colloid Interface Sci.* **1992**, *39*, 299.
(57) van Oss, C. J.; Good, R. J.; Busscher, H. J. *J. Dispersion Sci. Technol.* **1990**, *11*, 75−81.
(58) Battino, R.; Rettich, T. R.; Tominaga, T. *J. Phys. Chem. Ref. Data* **1983**, *12*, 163−178.

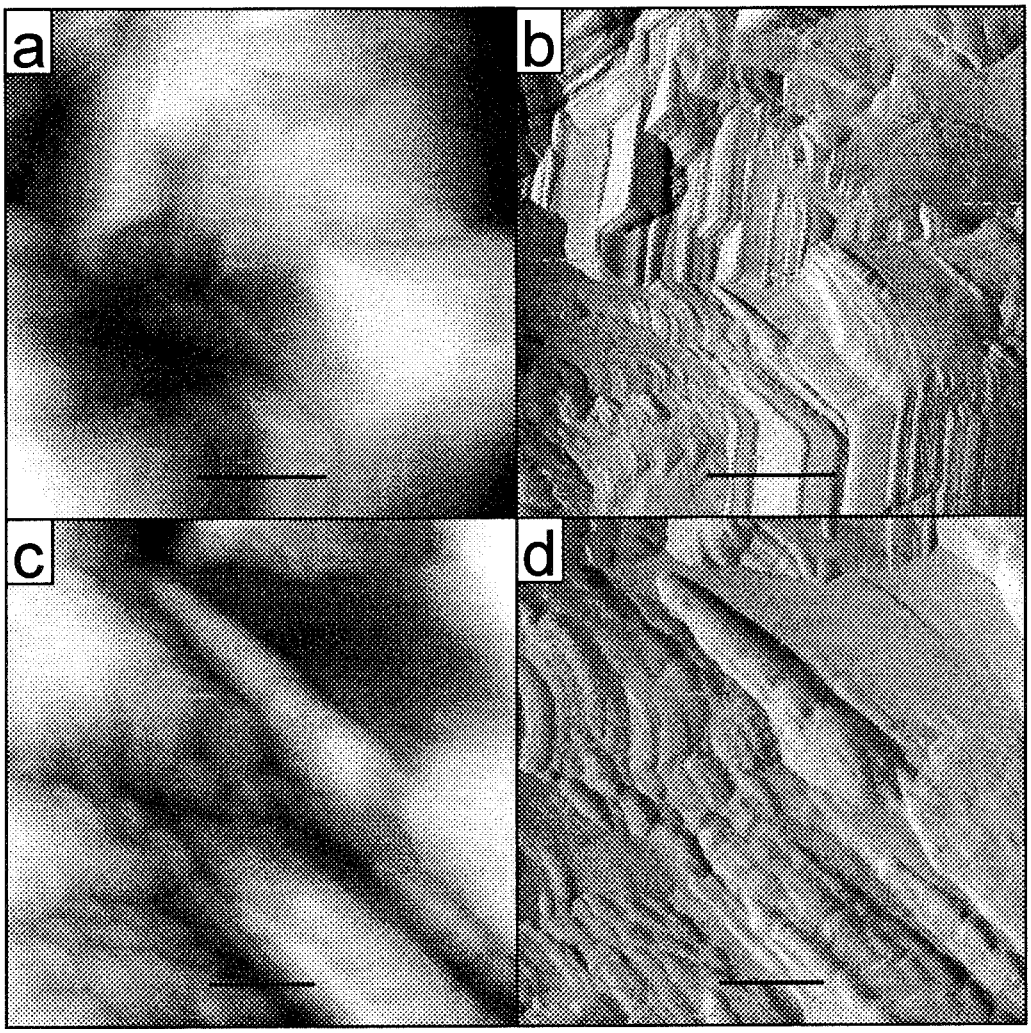

Figure 7. AFM height and corresponding tip deflection images of scribed Si. In larger area height (a) and deflection (b) images, the scale bar represents 2 μm. Crystalline facets can be observed in the bottom central and upper left regions. In zoomed height (c) and deflection (d) images, the scale bar denotes 500 nm. A relatively flat region is observed in the upper right portion of these images. Height scale is 2.5 μm in (a) and 500 nm in (c); deflection scale is 0.3 V in (b) and 0.1 V in (d). Areas of greater height or deflection correspond to lighter regions in the images.

underivatized interior regions of hydrophobic corrals can be selectively functionalized, and not the surrounding regions or neighboring corrals. (Liquids in adjacent corrals on gold were previously shown[28] not to communicate with each other.)

In polyelectrolyte deposition it is believed that an electrostatic attraction between a surface and a solvated polyelectrolyte drives film formation and that an electrostatic repulsion between adsorbed polymer chains and those in solution limits deposition to essentially monolayer quantities.[59,60] In brief (for a more detailed explanation see the Experimental Section) a droplet of water is put in a hydrophobic corral. Part of the droplet is then removed and replaced by a polymer solution to give a certain concentration above the surface. After a given amount of time to allow polelectrolyte deposition, the region is rinsed by repeatedly removing some of the liquid from the drop and replacing it with water. The next polyelectrolyte layer is then deposited by replacing some of the water in the droplet in the corral with a different polymer solution. In this manner polyelectrolyte multilayers are deposited in the interior regions of hydrophobic corrals.

Polyelectrolyte adsorption, using PSS and PAH, was followed with variable-angle spectroscopic ellipsometry. Because the optical constants for SiO_2 and most organics are very similar[40,41] and ellipsometry is quite insensitive to changes in optical constants of very thin films (<50 Å),[61] the adsorbed polymer and silicon oxide layers could be modeled as a single layer of silicon oxide on silicon using tabulated optical constants for these materials (see Figure 11).[40,41] The thickness of the initial sticking layer of poly(ethylenimine) (PEI) and silicon oxide was subtracted from the total film thicknesses giving 10.3 ± 0.5 and 17.4 ± 0.5 Å for PSS/PAH and $(PSS/PAH)_2$ multilayers, respectively. The thicknesses of two surfaces containing single PEI layers, which were deposited in the interior regions of hydrophobic corrals by the method described here, were measured with spectroscopic ellipsometry to be 3.8 and 3.9 Å. XPS confirmed the presence of nitrogen in these PEI layers.

C. Mathematical Analyses of Drop Shapes and Wetting in Hydrophobic Corrals. This section contains two mathematical treatments of liquid droplets in hydrophobic corrals. First, two finite element analyses of 20 μL water and methanol droplets in 0.5×0.5 cm^2

(59) Lvov, Yu.; Decher, G.; Möhwald, H. *Langmuir* **1993**, *9*, 481−486.

(60) Lvov, Yu.; Decher, G.; Haas, H.; Möhwald, H.; Kalachev, A. *Physica B* **1994**, *198*, 89−91.

(61) Tompkins, H. G. *A User's Guide to Ellipsometry*; Academic Press: San Diego, CA, 1993.

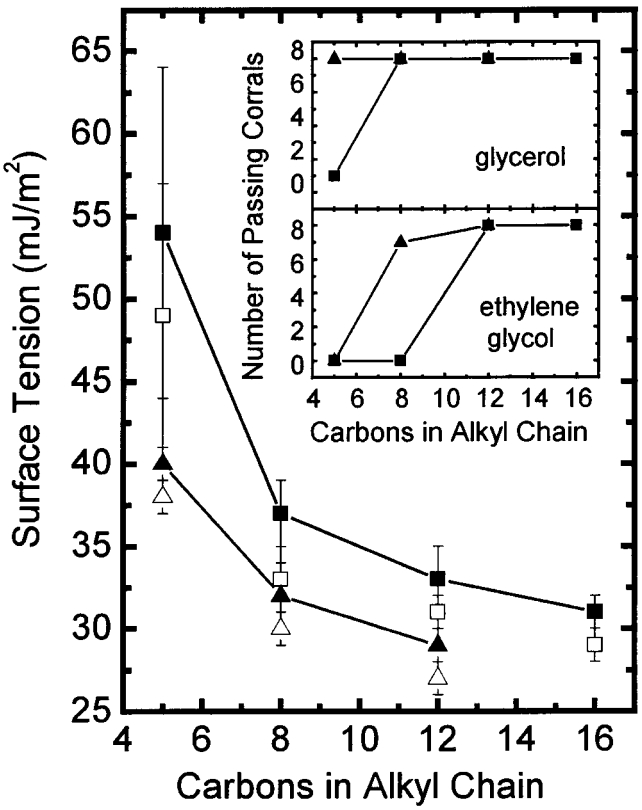

Figure 8. Passing (solid symbols) and failing (open symbols) surface tensions of 20 μL methanol−water test droplets in hydrophobic corrals made from 1-alkenes (squares) and 1-alkynes (triangles). The insets show the number of hydrophobic corrals out of eight tested, which held droplets of glycerol and ethylene glycol.

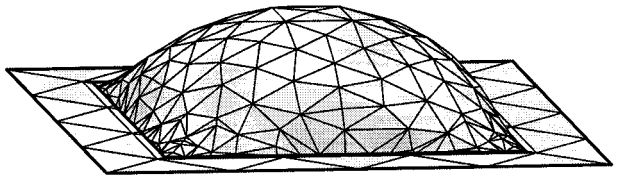

Figure 9. Finite element analysis of a 20 μL drop of water constrained to wet the interior of a 0.5 × 0.5 cm^2 square hydrophobic corral. The "drop" was first modeled as a parallelepiped and then triangulated. The first refinement of 1000 iterations had 58 vertexes, 152 edges, and 96 facets and was followed by a second refinement of 200 iterations with 234 vertexes, 648 edges, and 416 facets (shown).

hydrophobic corrals are described, and the resulting energies (surface and gravitational) for the droplets are given. Next is an analysis of drop failure in hydrophobic corrals, which yields a formula for $\gamma_{\text{line-air}} - \gamma_{\text{line-liquid}}$ (the difference between the surface tensions at the hydrophobic line/air interface and at the hydrophobic line/liquid interface).

Figure 9 shows the results of a finite element analysis of a 20 μL water droplet in a 0.5 × 0.5 cm^2 square hydrophobic corral with 234 vertexes, 648 edges, and 416 facets, which was performed with the Surface Evolver program (see Experimental Section). After a more thorough analysis, including multiple refinements and iterations, drops with 311 554 vertexes, 901 376 edges, and 589 824 facets had total energies (gravitational and surface) of 24.3174 ± 0.0001 and 7.9290 ± 0.0001 erg for water and methanol, respectively.

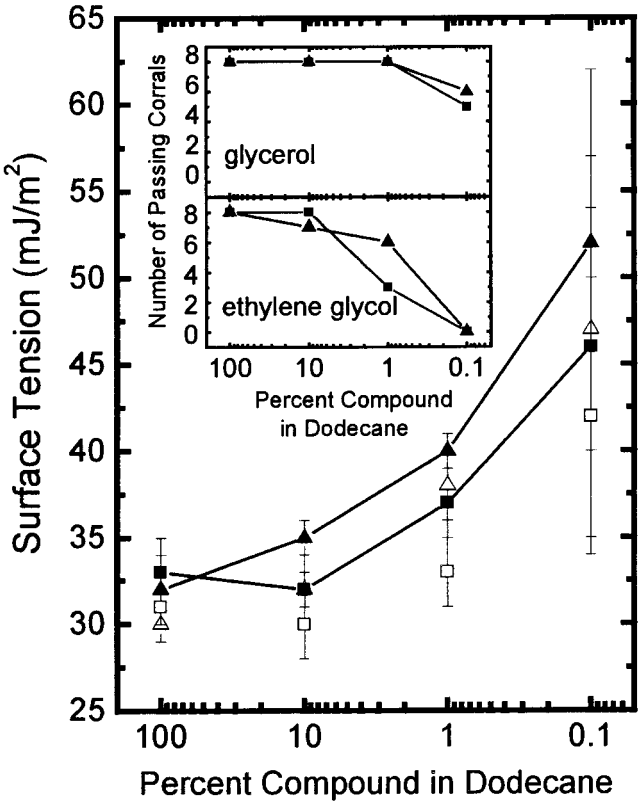

Figure 10. Passing (solid symbols) and failing (open symbols) surface tensions of 20 μL methanol−water test droplets in hydrophobic corrals made from 1-dodecene (squares) and 1-octyne (triangles), which were diluted in dodecane. The insets show the number of hydrophobic corrals out of eight tested, which held droplets of glycerol and ethylene glycol.

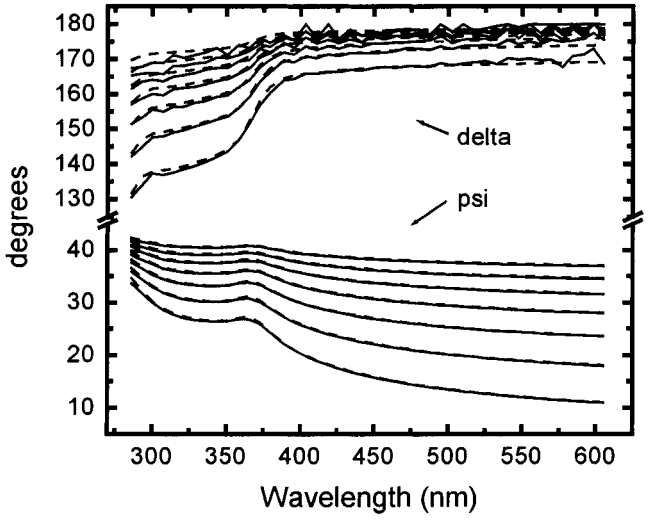

Figure 11. Variable angle spectroscopic ellipsometry data of a polyelectrolyte multilayer on oxidized silicon, i.e., silicon/silicon oxide/polyethylenimine/(poly(styrene sulfonate)/poly(allylamine) hydrochloride)$_2$. The solid lines are the experimental data and the dashed lines are the best fit, based on a model of 34.6 Å of silicon oxide on 1 mm of silicon, obtained using the instrument software. The sample was probed at different angles of incidence from 40° (top Ψ and Δ curves) to 70° (bottom Ψ and Δ curves) in steps of 5°.

While the Surface Evolver program can provide extremely accurate results, it is computationally expensive and fairly complicated to learn. The following function

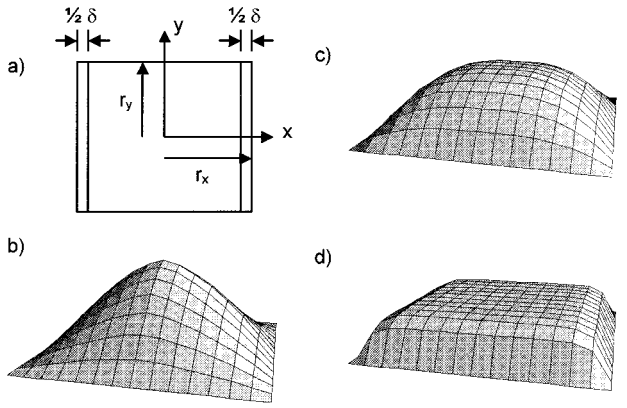

Figure 12. (a) Coordinate system on the base of a hydrophobic corral. $r_x > r_y$ if a droplet has penetrated a hydrophobic line in a square hydrophobic corral. (b–d) Plots of eq 3 with $r_x = r_y = 0.5$ cm for (b) $n = 1.5$, $h_n = 0.2222$ cm, (c) $n = 2.9758$, $h_n = 0.1428$ cm, and (d) $n = 10$, $h_n = 0.0968$ cm. h_n is the height of the drop at its center and $n = 2.9758$ minimizes the function with respect to energy (surface and gravitational) for water.

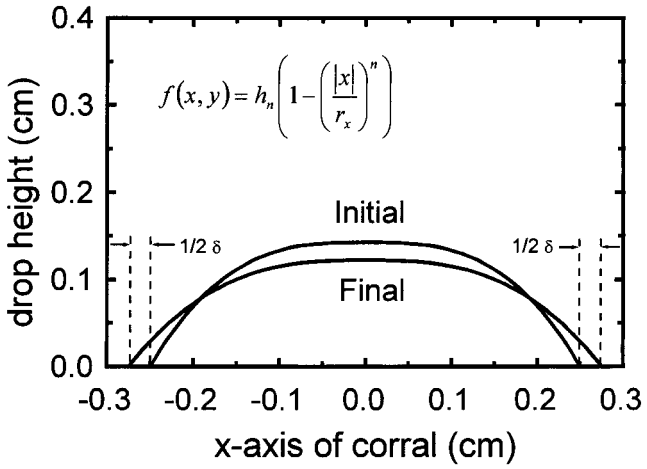

Figure 13. Profiles of two water droplets along the x axis in hydrophobic corrals. Values of n and h_n for the initial ($n = 2.9758$, $h_n = 0.1428$ cm, 0.5×0.5 cm^2) and final ($n = 2.8183$, $h_n = 0.1224$ cm, 0.5×0.55 cm^2) states minimize the droplet energies.

was found to closely approximate the shapes of 20 μL droplets of liquids in 0.5×0.5 cm^2 hydrophobic corrals:

$$f(x,y) = h_n\left(1 - \left(\frac{|x|}{r_x}\right)^n\right)\left(1 - \left(\frac{|y|}{r_y}\right)^n\right) \quad (3)$$

The origin ($x = y = 0$) (see Figure 12a) for this function is placed at the center of a corral and the x and y axes run perpendicular to the sides of a hydrophobic corral. r_x and r_y are distances from the origin to the edge of the corral in the x and y directions, and h_n is the height of the function at the origin. The liquid surface tension, density, and total volume were inputs for a Mathematica program (see Supporting Information), which was written to calculate the surface area of a droplet's liquid–air interface and its center of mass, from which its gravitational energy was obtained. The program finds the value of the adjustable parameter, n, that minimizes the sum of the surface and gravitational energies.

Figure 12b–d shows 20 μL droplets in 0.5×0.5 cm^2 hydrophobic corrals for different values of n as predicted by eq 3. For small n, the function is peaked at the origin, and for large n, the function has a broad, flat top and begins to approximate a parallelepiped. Minimization of the overall energy for 20 μL droplets of pure water and pure methanol gives the following values of n, the total energy, the surface energy, and the gravitational energy: 2.9758 ± 0.0001, 24.4066 ± 0.0001 erg, 23.3839 ± 0.0001 erg, 1.0227 ± 0.0001 erg; 3.3708 ± 0.0001, 7.9681 ± 0.0001 erg, 7.1829 ± 0.0001 erg, 0.7852 ± 0.0001 erg, respectively. These total energies for methanol and water are within 0.5% of those predicted by the more thorough finite element analysis. Results from this function are expected to decrease in accuracy as the drop volume increases because it cannot account for contact angles greater than 90°. As expected, the surface energy component for water droplets is much greater than that for methanol droplets. The larger value of n for methanol is a reflection of its lower surface tension, which allows gravity to deform methanol droplets more than water droplets when they are pinned in hydrophobic corrals.

By use of eq 3, a formula was obtained that relates failure of a hydrophobic corral to hold a droplet of some liquid to the difference between the surface tensions of the hydrophobic line–air interface and the hydrophobic line–water interface: $\gamma_{\text{line-air}} - \gamma_{\text{line-liquid}}$. This expression is the analogue of $\gamma_{SV} - \gamma_{SL}$ in Young's equation, $\gamma_{SV} - \gamma_{SL} = \gamma_{LV}\cos\theta$, where γ_{SV}, γ_{SL}, and γ_{LV} are the surface tensions of the surface–vapor (SV), surface–liquid (SL), and liquid–vapor (LV) interfaces and θ is the contact angle of a droplet on a surface. $\gamma_{SV} - \gamma_{SL}$ is the most relevant output of Young's important equation because θ is measurable and γ_{LV} is generally available, while γ_{SV} and γ_{SL} are usually unknown.[62]

Figure 13 shows the profile of a liquid droplet in a hydrophobic corral along the x axis (see Figure 12) both before (initial) and after (final) spreading some distance into a hydrophobic corral. As can be seen in Figure 13, the center of mass of the drop decreases when it spreads, reducing the gravitational energy of the drop. However, after the drop has spread, the surface area at the drop's air–liquid interface increases, raising the surface energy of the drop. For 20 μL droplets in hydrophobic corrals with surface tensions that range from methanol to water, the increase in energy due to an increase in air–liquid surface area is greater than the decrease in gravitational energy. Thus an additional driving force, which we show to be $\gamma_{\text{line-air}} - \gamma_{\text{line-liquid}}$, must be present for a drop to wet a hydrophobic line, i.e., fail to be held by a hydrophobic corral.

For a droplet in a hydrophobic corral, we obtain the following expressions for its initial (E_i) and final (E_f) energies, before and after it spreads into a hydrophobic line

$$E_i = E_{i,\text{gravitational}} + E_i(\gamma_{\text{air-liquid}}) + E_i(\gamma_{\text{interior surface-liquid}}) + E_i(\gamma_{\text{line-liquid}}) + E_i(\gamma_{\text{line-air}}) \quad (4)$$

$$E_f = E_{f,\text{gravitational}} + E_f(\gamma_{\text{air-liquid}}) + E_f(\gamma_{\text{interior surface-liquid}}) + E_f(\gamma_{\text{line-liquid}}) + E_f(\gamma_{\text{line-air}}) \quad (5)$$

Here, $E_{i,\text{gravitational}}$ and $E_{f,\text{gravitational}}$ are the gravitational energies of the drop before and after spreading into the hydrophobic line. $E_i(\gamma_{\text{air-liquid}})$ and $E_f(\gamma_{\text{air-liquid}})$ are the surface contributions to the total energy from the air–liquid interface of the drop. $E_i(\gamma_{\text{interior surface-liquid}})$ and $E_f(\gamma_{\text{interior surface-liquid}})$ are the surface energies from the interior surface of the hydrophobic corral and the liquid drop, which are equal because the interior region of the hydrophobic corral is wet by the liquid before and after

(62) de Gennes, P. G. *Rev. Mod. Phys.* **1985**, *57*, 827–863.

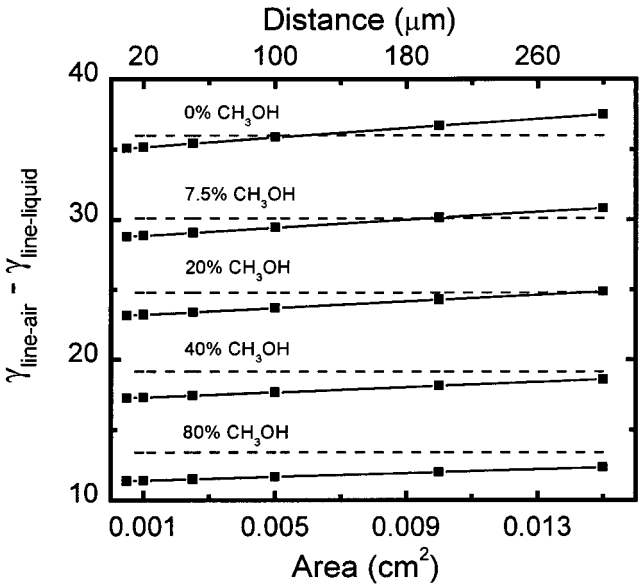

Figure 14. Difference between the line−air surface tension ($\gamma_{\text{line-air}}$) and line−liquid surface tension ($\gamma_{\text{line-liquid}}$) as a function of the area a droplet penetrates a hydrophobic line.

spreading (see Figure 13). The remaining terms are defined in terms of the area, A, that the drop penetrates into a hydrophobic line. $E_i(\gamma_{\text{line-liquid}})$ and $E_f(\gamma_{\text{line-liquid}})$ are the surface energies associated with the hydrophobic line−liquid interface, and $E_i(\gamma_{\text{line-air}})$ and $E_f(\gamma_{\text{line-air}})$ are the energies associated with the hydrophobic line−air interface. Initially, the drop has not spread into the line so $E_i(\gamma_{\text{line-liquid}}) = 0$ and $E_i(\gamma_{\text{line-air}}) = A\gamma_{\text{line-air}}$. After the drop has spread, $E_f(\gamma_{\text{line-liquid}}) = A\gamma_{\text{line-liquid}}$ and $E_f(\gamma_{\text{line-air}}) = 0$. The change between the initial and final energies of these systems is defined to be $\Delta E = E_f - E_i$. We also define $\Delta E_{\text{gravitational}} = E_{\text{f,gravitational}} - E_{\text{i,gravitational}}$ and $\Delta E(\gamma_{\text{air-liquid}}) = E_f(\gamma_{\text{air-liquid}}) - E_i(\gamma_{\text{air-liquid}})$. These definitions and results yield the following expression for ΔE:

$$\Delta E = \Delta E_{\text{gravitational}} + \Delta E(\gamma_{\text{air-liquid}}) + A\gamma_{\text{line-liquid}} - A\gamma_{\text{line-air}} \quad (6)$$

A minimal condition for wetting of a hydrophobic line by a liquid in a hydrophobic corral is $\Delta E = 0$, which reduces eq 6 to

$$\gamma_{\text{line-air}} - \gamma_{\text{line-liquid}} = \frac{\Delta E_{\text{gravitational}} + \Delta E(\gamma_{\text{air-liquid}})}{A} \quad (7)$$

A Mathematica program (see Supporting Information) was run to calculate $\Delta E_{\text{gravitational}} + \Delta E(\gamma_{\text{air-liquid}})$ for droplets of liquids with different surface tensions in hydrophobic corrals before and after they spread some amount into a hydrophobic line. For simplicity, it was assumed that the entire front of the drop moved a certain distance (δ, see Figure 12) into a hydrophobic line, that the scribed line is smooth, and that the contact angle of the drop is given by eq 3. In this analysis, an excursion of $^1/_2\delta$ on either side of a hydrophobic corral is mathematically equivalent to an excursion of δ on one side of a hydrophobic corral and the calculations were run in the former manner, taking advantage of the symmetry of that geometry (see Figure 12).

Figure 14 shows the results (solid squares) of this simulation for different concentrations of methanol in water. As expected, low percentages of methanol in water require a higher driving force ($\gamma_{\text{line-air}} - \gamma_{\text{line-liquid}}$) than higher percentages of methanol in water, which have lower surface tensions. Also, as the excursion of the droplet into the hydrophobic line increases, $\gamma_{\text{line-air}} - \gamma_{\text{line-liquid}}$ also increases, again indicating that an increasingly greater driving force is necessary to deform the drop. These results are in agreement with the earlier observation that wide functionalized lines on gold are better barriers to liquid droplets than narrower boundaries.[28] The dashed horizontal solid lines in Figure 14 are equal to $^1/_2\gamma_{\text{air-liquid}}$ for each liquid, suggesting that $\gamma_{\text{line-air}} - \gamma_{\text{line-liquid}} \approx {}^1/_2\gamma_{\text{air-liquid}}$ is a fair estimate for the excursion of a droplet 50−100 μm into a hydrophobic line. Thus, for the problem at hand, this analysis suggests that approximately half of the average of the passing and failing surface tensions of methanol−water droplets in a given hydrophobic corral (see Figure 8) is equal to $\gamma_{\text{line-air}} - \gamma_{\text{line-liquid}}$. In contrast, for complete wetting, where $\theta = 0$, Young's equation gives $\gamma_{SV} - \gamma_{SL} = \gamma_{LV}$ or $\gamma_{\text{line-air}} - \gamma_{\text{line-liquid}} = \gamma_{\text{air-liquid}}$.

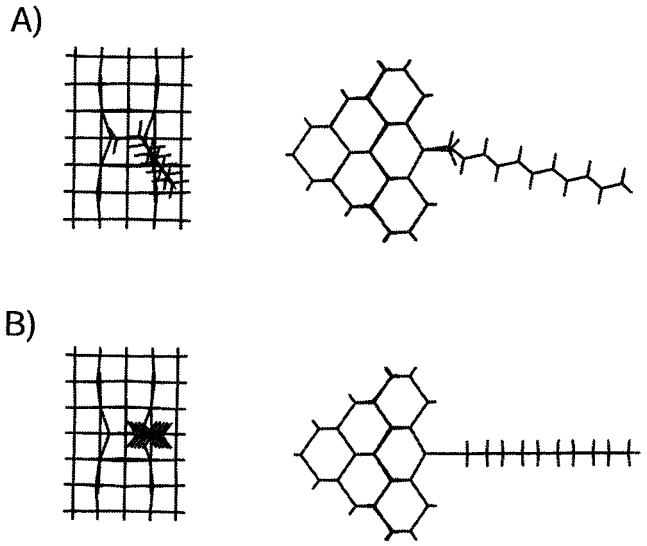

Figure 15. (A) Theoretical results using a Hartree−Fock 3-21G* basis set for 1-dodecene and (B) 1-dodecyne covalently bonded to a silicon cluster. The carbon atoms from the double or triple bond are each bonded to a silicon atom and the degree of unsaturation of the adsorbed species has decreased upon binding; i.e., the 1-alkene-derived adsorbate is saturated and the 1-alkyne-derived adsorbate has a double bond (see Figure 2 for proposed binding of a 1-alkene).

D. Theoretical Modeling of Unsaturated Species on Silicon. The XPS data presented here (see Figure 4) show that 1-alkenes and 1-alkynes with the same chain length form thin films on scribed silicon that have the same amount of carbon (C 1s/Si 2p ratio). However, wetting data (see Figure 8) indicate that monolayers derived from 1-alkynes are more hydrophobic than those produced from 1-alkenes. While we have not determined the mechanism of binding of alkyl chains to silicon in this work, one possible explanation for these results is a difference in orientation between alkyl tails of 1-alkenes and 1-alkynes that might bind to silicon by a [2 + 2] addition mechanism (see Figure 2 and the Introduction).

Figure 15, Table 1, and Table 2 show results of molecular mechanics, semiempirical, and ab initio quantum calculations[15,24,26] of 1-dodecene and 1-dodecyne bonded to the (100) face of a silicon cluster with 48 silicon atoms through two carbon−silicon bonds. A covalent bond links the two silicon atoms that these carbons are bonded to (see Figure 2), and the alkyl chains are numbered consecutively starting at the unsaturated end of the chain, with C(1) bonded to Si(1), and C(2) to Si(2). Figure 15 clearly shows that the alkyl chain in 1-dodecene tilts significantly (note

Table 1. Theoretical Calculations of 1-Dodecene Chemisorbed on Si(100) through Two Carbon−Silicon Bonds (See Figures 2 and 15)[a]

	MMFF94	PM3	STO-3G	3-21G*
C(1)−Si(1)−Si(2)−C(2) dihedral angle	19.22	9.32	9.38	5.91
Si(1)−C(1)−C(2)−C(3) dihedral angle	154.77	133.54	133.64	137.34
C(1)−C(2)−C(4)−90° angle	8.36	9.99	9.95	8.20
C(2)−C(4)−C(6) angle	178.82	179.32	179.27	179.48
C(1)−C(2)−C(3) angle	114.96	115.78	115.77	114.46
C(1)−Si(1)	1.866	1.913	1.913	1.903
C(2)−Si(2)	1.891	1.939	1.938	1.918
Si(1)−Si(2)	2.585	2.399	2.399	2.352
C(1)−C(2)	1.563	1.501	1.502	1.582
C(2)−C(3)	1.536	1.508	1.508	1.548
C(3)−C(4)	1.532	1.522	1.522	1.547

[a] Units of numbers in the table are either degrees for angles or angstroms for distances, as appropriate. Carbons are numbered from the unsaturated end of the alkyl chain. Si(1) is bonded to C(1) and Si(2) to C(2).

Table 2. Theoretical Calculations of 1-Dodecyne Chemisorbed on Si(100) through Two Carbon−Silicon Bonds (See Figure 15)[a]

	MMFF94	PM3	STO-3G	3-21G*
C(1)−Si(1)−Si(2)−C(2) dihedral angle	−0.03	−0.04	−0.072	0.00
Si(1)−C(1)−C(2)−C(3) dihedral angle	−179.92	−179.88	−179.88	−179.99
C(1)−C(2)−C(4)−90° angle	7.36	7.27	7.28	5.11
C(2)−C(4)-C(6) angle	179.34	177.71	177.74	178.09
C(1)−C(2)-C(3) angle	129.76	130.79	130.79	127.66
C(1)−Si(1)	1.856	1.837	1.837	1.871
C(2)−Si(2)	1.893	1.859	1.860	1.888
Si(1)−Si(2)	2.529	2.439	2.439	2.253
C(1)−C(2)	1.363	1.331	1.330	1.328
C(2)−C(3)	1.581	1.472	1.472	1.532
C(3)−C(4)	1.526	1.522	1.521	1.546

[a] Units of numbers in the table are either degrees for angles or angstroms for distances, as appropriate. Carbons are numbered from the unsaturated end of the alkyl chain. Si(1) is bonded to C(1) and Si(2) to C(2).

the Si(1)−C(1)−C(2)−C(3) dihedral angle in Table 1 and also that different chains would be expected to tilt to the right or to the left depending on how they are attached to the surface), while the alkyl chain of 1-dodecyne does not tilt appreciably (note the Si(1)−C(1)−C(2)−C(3) dihedral angle in Table 2). Another measure of tilt, which is about the same for both adsorbed species, is the C(1)−C(2)−C(4) angle minus 90°, where the vector connecting C(2) and C(4) is essentially the chain axis because the angle C(2)−C(4)−C(6) is nearly equal to 180° for the different chains (see Tables 1 and 2). Every level of theory that these systems were examined with supports these general conclusions. Thus, alkyl chains in monolayers of 1-alkenes, if bonded as shown in Figure 15, are expected to have more difficulty packing than alkyl chains from 1-alkynes. They would further be expected to expose more methylene units at their surfaces than monolayers of 1-alkynes and therefore have higher surface tensions,[50] as is observed here (see Figure 8).

The bond distances predicted by the different levels of theory in Tables 1 and 2 are in good agreement, as has been observed in theoretical calculations of bonding between second- and third-row elements in a wide variety of compounds.[63] However, the bond angles sometimes differ substantially, even between the STO-3G and 3-21G* Hartree−Fock basis sets. The 3-21G* basis set is assumed to produce more accurate results because it incorporates d orbital type functions, while the STO-3G is a minimal basis set that does not. For 1-dodecene (Table 1) the C(1)−Si(1)−Si(2)−C(2) and Si(1)−C(1)−C(2)−C(3) dihedral angles change from 9.38° and 133.64° (STO-3G) to 5.91° and 137.34° (3-21G*), respectively. For 1-dodecyne (Table 2) the C(1)−C(2)−C(4)−90° angle changes substantially going from the STO-3G (7.28°) to the 3-21G* basis set (5.11°). Overall, the results of the different levels of theory are more consistent for the 1-dodecyne system than for that of 1-dodecene, probably because of the higher symmetry of the 1-dodecyne/silicon cluster.

Conclusion

These results show a new and facile preparation of monolayers on silicon, which only requires some inexpensive and easily obtainable equipment and reagents. With this method, enclosures, which partition the surface into separate regions, can be prepared and initial results suggest that separate regions on silicon can be selectively functionalized. Such arrays may be useful in preparing combinatorial libraries of small molecules and polymers and in optimizing surface reactions. Because surface dimers analogous to those on Si(100) form on unpassivated diamond(100) and germanium(100) and these species are known to react with alkenes and dienes,[15,64−67] we expect it will be possible to use this scribing method to functionalize these materials. It may also be possible to similarly derivatize glass (quartz) and polymer surfaces. By reducing the pressure on and/or decreasing the size of the tip of the scribe (even down to the dimensions of an AFM or STM tip), it should be possible to create much smaller features than were demonstrated here. In the case of reactive monomers with no allylic hydrogen and where limited oxygen and/or inhibitors are present, polymerization may occur. It may also be possible for alkynes to form more than two C−Si bonds to the surface.[26]

Acknowledgment. We thank Jennifer McBride, Yingjie Zhu, and Robert Hirsch for their help in collecting XPS and TOF-SIMS data on instruments purchased with NSF Grant DMR-9724307 at the Surface Analysis Facility at the University of Utah, Robert Perry at the BYU Precision Machining Laboratory for writing the program that controlled the CNC, Michael Standing for collecting SEM data, Philroy Brown for helping with the profilometry, and Patrick Schnabel for a useful suggestion.

Supporting Information Available: A Mathematica notebook with code and documentation for calculating drop energies using eq 3 and files of the theoretical calculations of 1-dodecene and 1-dodecyne on silicon clusters in Brookhaven Protein Database (pdb) format. This material is available free of charge via the Internet at http://pubs.acs.org.

Note Added after ASAP Posting. This article was released ASAP on 8/23/2001 with an error in equation 1. The correct version was posted on 9/11/2001.

LA010017A

(63) Hehre, W. J.; Yu, J.; Klunzinger, P. E.; Lou, L. *A Brief Guide to Molecular Mechanics and Quantum Chemical Calculations*; Wavefunction, Inc.: 1998.

(64) Fitzgerald, D. R.; Doren, D. J. *J. Am. Chem. Soc.* **2000**, *122*, 12334−12339.

(65) Hamers, R. J.; Hovis, J. S.; Greenlief, C. M.; Padowitz, D. F. *Jpn. J. Appl. Phys.* **1999**, *38*, 3879−3887.

(66) Hovis, J. S.; Coulter, S. K.; Hamers, R. J.; D'Evelyn, M. P.; Russell, J. N., Jr.; Butler, J. E. *J. Am. Chem. Soc.* **2000**, *122*, 732−733.

(67) Teplyakov, A. V.; Lal, P.; Noah, Y. A.; Bent, S. F. *J. Am. Chem. Soc.* **1998**, *120*, 7377−7378.